Ultrasensitive, highly selective and real time detection of protein using functionalized CNTs as MIP platform for FOSPR based biosensor

Ultrasensitive, highly selective and real time detection of protein using functionalized CNTs as MIP platform for FOSPR based biosensor

Anisha Pathak, Shama Parveen, and Banshi D. Gupta*

Physics Department

Indian Institute of Technology Delhi

New Delhi-110016, India

---

*Corresponding author

Email: bdgupta@physics.iitd.ac.in

Phone: 91-11-26591355

Abstract

A facile approach is presented for the detection of Bovine serum albumin (BSA), based on fiber optic SPR (FOSPR) cooperated with molecular imprinting (MIP). The probe is fabricated by exploiting the plasmonic property of silver thin film and vinyl functionalised carbon nanotubes based MIP platform. BSA template molecules are imprinted on the MIP layer coated over multi-walled carbon nanotubes (MWCNTs) to ensure high specificity of the probe in the interfering environments. In addition, FOSPR endorses the sensor capability of real time and remote sensing along with very high sensitivity due to the use of nanostructured MIP platform. The response of the probe is considered in terms of absorbance spectrum recorded for various concentrations of BSA. The sensor shows a wide dynamic range of 0-350 ng/L with a considerably linear response up to 100 ng/L in peak absorbance wavelength with BSA concentration. Highest sensitivity of 0.862 nm/ngL^{-1} is achieved for the lowest concentration of BSA and it decreases with the increase in BSA concentration. The performance of the present sensor is compared with those reported in the literature in terms of limit of detection (LOD). It is found that the probe possesses lowest LOD of 0.386 ng/L in addition to other advantages like real time online monitoring, high sensitivity, high specificity and remote sensing.

Key words: Sensor, protein, carbon nanotube, optical fiber, surface plasmon, molecular imprinting

Introduction

Various areas of life sciences demand for the qualitative and quantitative determination of essential biological compounds such as protein which is an important constituent of cell. The perceptible determination of protein has numerous applications in the fields of nutrition, pharmacology and biotechnology [1]. Among the various proteins, albumin is abundant in vertebrate blood and is used as carrier protein for many endogenous and exogenous compounds in the blood, extract oxygen free radicals and maintenance of osmotic homeostasis of blood. Bovine serum albumin (BSA) is one of the most extensively studied proteins in the serum family having 582 amino acids residues with 17 cysteine cross-linked residues and 1 free cysteine [2,3]. Multiple abundant functional elements attached with BSA make it a multifunctional protein for the delivery of fatty acid/amino acid and binding etc. Its uniquely stable and non-interfering structure make it vital in various biochemical reactions such as enzymatic reactions, cell culture, ELISAs (enzyme-linked immunosorbent assay), immunoblots, immune histochemistry, protein concentration standard and assay standards. BSA is also a common additive for PCR (Polymerase Chain Reactions) amplifications, foot printing and gel shift assays [4]. These vast applications make the determination of BSA very important for the areas like drug delivery, medical diagnosis and monitoring bioterrorism. The challenge in the domain of proteins detection is their real time monitoring at extremely low concentrations with minimum requirement of sample preparation/labelling. Real time monitoring is important with the aspect of studying binding kinetics, specificity and affinity [5]. Over the years, many methods like colorimetric assays [6], surface enhanced Raman spectroscopy [7], NIR reflectance spectroscopy [8], fluorimetry [9] and spectrophotometry [10] have been reported for the detection of BSA but with limited sensitivity and selectivity. Thus, in this study, we provide a method for accurate detection of BSA which can meet with all the above requirements like real time monitoring at low concentrations, no sample preparation, and high specificity. The method is based on combination of surface plasmon resonance technique and optical fiber technology along with molecular imprinting of BSA molecules on the surface of carbon nanotubes.

In molecular imprinting (MI) technology, specific recognition cavities of a template molecule are created in artificial materials like synthetic polymers by the means of copolymerisation of monomers and cross-linkers [11]. The recognition sites are made by removal of template after the copolymerisation step and hence are highly complementary to the template molecules in terms of shape, size and functional groups attached. Thus, molecular imprinting is a widely

acceptable, promising and facile technique for the mimic of biological receptors like antibody-antigen, enzymes etc. Molecularly imprinted polymers are much more stable and economic as compared to their biological counterparts [4]. Hence, the technique has gained enormous research interest in various fields like separation, analytical chemistry, catalysis and specifically biosensing [12]. Ever since its discovery [13, 14], MI technology has been limited to the detection of small molecules with great success. However, the technology has also been explored for the macromolecules like proteins due to their 3D structural conformation, complexity, solubility and large molecular size. Moreover, the diffusion limitation of proteins makes their uptake and removal cumbersome in imprinting leading to decrease in sensitivity [15,16]. To overcome this limitation, nanotechnology has opened a feasible strategy for an improvised version of MI called as surface imprinting. Some of the very early applications of surface imprinting were illustrated for proteins [17, 18]. In surface imprinting, the recognition sites complementary to the template molecules are created on the surface of a nanostructure. The binding sites available on the surface make the binding and removal of template easier and more accessible with quicker response. Many nanostructured matrices have been proposed over the time for MI such as silica nanoparticles, graphene, polymer microspheres and CNTs [15]. Multi-walled carbon nanotubes (MWCNTs) have been the nanomaterial of choice in many versatile areas. They are considered as an ideal supporting material because of their unique geometry with high surface to volume ratio, appreciable electrical and optical properties with good chemical stability and robustness. MWCNTs have been widely used by numerous groups for surface imprinting due to their unique properties [19-21]. Compared with MWCNTs, carboxyl functionalized MWCNTs (MWCNTs-COOH) have better and stable dispersion ability, binding ability and strength [21]. They can serve as a robust support as a core material in core-shell type MIPs like the one reported here.

In this work we report a core@shell nanostructure i.e MWCNTs@MIP composites for protein detection by using BSA as a template molecule and copolymerization of vinyl end on the surface of CNTs over Ag coated fiber core. The overall approach relies on the MI technique and fiber optic surface plasmon resonance [22, 23]. In SPR based sensors, the resonance condition depends on the refractive index of the dielectric layer in the vicinity of the metal. Thus, as the refractive index of MIP layer around the silver layer changes due to the binding of template molecule, the resonance condition of SPR changes which can be read by means of change in the resonance parameter (wavelength in this case) [24]. Moreover, the

use of optical fiber as a versatile platform adds many advantages like remote sensing and online monitoring capability, geometric versatility, small size and weight. The characterization of the proposed MIP/SPR fiber optic sensing probe has been carried out for lower concentrations of BSA from 0-350ng/L. In addition, the effect of pH on the performance of the sensor has been evaluated. To check the selectivity of the probe, measurements have been carried out on different types of analyte solutions such as HSA (human serum albumin), BHb (Bovine Haemoglobin), urea, glucose and dopamine which have similar structure as BSA and can interfere with its detection. The optimization of the concentration of BSA used for the fabrication of probe and other MIP parameters for the best performance of the sensor have also been carried out.

Experimental

Chemicals and Apparatus

Plastic clad silica (PCS) optical fiber having 600 µm core diameter and 0.4 numerical aperture was purchased from Fiberguide Industries (USA). Multiwall carbon nanotubes (MWCNTs) were purchased from SRL Pvt. Ltd. Nitric acid, ammonium hydroxide and (3-mercaptopropyl) trimethoxy silane (MPTS) were purchased from Sisco Research Laboratories (India) for functionalization and vinyl attachment. For the preparation of molecular imprinting polymer, methacrylic acid (MAA) and ethylene glycol dimethacrylate (EGDMA) used as monomer and cross-linker, respectively, were purchased from Merck Specialties Pvt. Ltd. 2-2-Azobisisobutyronitrile (AIBN) used as an initiator was purchased from Otto Kemi. Methanol used for the removal of template molecules from the polymer was purchased from Fisher Scientific. Sodium dihydrogen phosphate dihydrate (NaH_2PO_4:$2H_2O$) and disodium hydrogen phosphate dihydrate (Na_2HPO_4:$2H_2O$) were purchased from Merck India for the preparation of phosphate buffer solution. DI Water used for the preparation of different kinds of samples was purchased from Millipore® System. For selectivity tests HSA, BHb, urea, glucose and dopamine were purchased from Sigma Aldrich Pvt. Ltd. Silver (Ag) wire (99.99% pure) was purchased from a local vendor.

For the coating of Ag thin films over the unclad core of the fiber, HINDHIVAC coating unit (model: 12A4D) was used. Abbe refractometer having resolution of 0.001 was used to measure the refractive index of various BSA solutions. To characterize the optical fiber probes, a tungsten halogen lamp (model: AvaLight-HAL) was used as source and a spectrometer (model: Avaspec-3648) was used for the recording of the transmittance spectra. Scanning electron microscopy of the MWCNTs and molecularly imprinted MWCNTs was performed using ZEISS EVO series (model: EVO 50) scanning electron microscope (SEM).

Preparation of stock solution

BSA solutions in the concentration range from 0 to 350 ng/L were prepared for the characterization of sensing probes. A stock solution was prepared by mixing 0.002 g of BSA in 100 ml of 0.01M (pH 7.0) phosphate buffer. The homogeneity of the stock solution was obtained by mixing the solution using homogenizer for 30 min in 2000 rpm mode. The solution was further sonicated for 20 min in ultra-sonicator. The sample solutions of different concentrations were prepared by simply diluting the above stock solution. The refractive indices of all the sample solutions were measured and found to be approximately same within the resolution of Abbe refractometer. BSA solutions of varying pH (5–9) were also prepared to check the effect of pH on the sensing probe. For the selectivity measurement, the solutions of different analytes were prepared in the similar manner.

Dispersion and Vinyl-functionalization of MWCNTs

10 mg of pristine MWCNTs were first dispersed into 20 ml of DI water using ultra-sonicate bath for 30 min. Uniform dispersion of MWCNTs was mixed with concentrated nitric acid at 60 °C under constant stirring for 2 h and further treated in ultra-sonicator for 30 min. After this, obtained black solution was diluted with DI water and rinsed for many times until the pH value reaches to neutral. The resulting modified MWCNTs with carboxylic group were filtered and separated from the solution. Finally, carboxylic group functionalized MWCNTs (MWCNT-COOH) were obtained by drying filtered solid under vacuum at 60 °C for further attachment of vinyl group [25]. Vinyl modification of MWCNTs makes compatible platform for MIP [19]. For vinyl modification, 2 mg dried powder of COOH-MWCNTs was dissolved in 10 mL of DI water and 1.5 mL of $NH_3.H_2O$ in a round bottomed flask by sonication for 30 min. The mixture obtained was stirred vigorously at 800 rpm for 2 hrs, whilst adding 300 mL of MPTS drop by drop. The above mixture was stirred further for 24 h at 60 °C. Treatment with MPTS imparts MWCNTs with vinyl groups as well as sulfonic groups due to oxidation of –SH group present [26, 27]. Vinyl group modified CNTs offer a compatible platform for the attachment of molecular imprinting polymerisation mixture [19] whereas, the vinyl sulfone group helps in the immobilisation of BSA over the CNTs surface [26-28]. The final product viz. vinyl-modified MWCNTs were filtered and washed with double distilled water many times [29]. To remove the interfering substance, filtered powder was washed by methanol and dried at 50 °C in vacuum.

Preparation of core-shell MWCNTs@BSA-MIP and MWCNTs@NIP

The synthesis of MWCNT@BSA molecularly imprinted polymer was performed as follows: 1 mg of above synthesized vinyl functionalised MWCNTs was mixed with a solution of BSA in phosphate buffer. The mixture was magnetically stirred at 600 rpm for 2 h. After that, the BSA-immobilized solution was washed three times with DI water to complete the reaction. Prepared complex was further mixed with 0.88 mM of MAA, 4.40 mM of EGDMA, 30 mg of AIBN, and 30 mL of acetonitrile under nitrogen gas flow for 30 min. The mixture was then left for polymerization at 40 °C for 12 h under constant magnetic stirring [30,31]. Nitrogen purging was carried out for removing the oxides from the polymerized solution. The schematic of MIP preparation is shown in figure 1(a). The template molecule, BSA with varying concentrations, 5-25 mg/L, were used for the optimization of BSA concentration in MWCNT@BSA-MIP layer. The range of sensor probe can be varied according to the BSA concentration used during probe fabrication. We have optimised the BSA concentration for the lower range of BSA detection i.e 0 to 350 ng/L.

Fabrication of probe

The sensing probes were fabricated in three steps. In the first step, a thin film of Ag was deposited over the unclad core of the fiber. In the second step, the Ag coated probes were coated with core shell MWCNT@BSA-molecular imprinting polymer/non-imprinted polymer (polymer with template molecule BSA/NIP) by dip coating method. The third step involves the creation of imprinted sites by removing the template molecules from the MIP layer using methanol/water. For the first step, cladding from about 1 cm portion of the 17 cm long PCS fiber from middle was removed using a sharp stainless steel blade. The unclad segment was then washed three times by water and ethanol successively. To remove further contamination on the unclad portion, fiber was further treated by ion bombardment process in vacuum at the chamber pressure of $5x10^{-2}$ mbar. Ultra cleaned probe was loaded in substrate holder attached in thermal evaporation system for the deposition of silver layer. Fiber core was then coated with a 40 nm thick Ag film at a vacuum pressure of $5x10^{-6}$ mbar. The deposition rate was fixed as 0.04 nm/sec. The uniform layer of Ag was achieved by rotating the fiber. The thickness and the deposition rate were monitored using a quartz crystal thickness monitor. This completes the first layer of the sensing probe. In the next step, dip coating method was employed for the coating of core-shell MWCNT@BSA MIP layer having BSA as template molecules over Ag coated probe. Ag coated portion of optical fiber was dipped vertically into cylindrical vessel filled with core-shell MIP solution prepared above. Coating of core-shell MIP layer was carried out for varying dipping time from 5 to 30 min. This was performed to optimize the dipping time of the sensing probe for the coating of

core shell MIP layer to achieve the best performance of the BSA sensor. Dipping time governs the optimum thickness of the MIP layer deposited over the Ag layer, which in turn is related to the overall sensitivity [32]. After removing the probe from the MIP solution it was left for 24 hrs at room temperature. This completed the second step of the probe fabrication. In the final step, template molecules (BSA) were removed from core shell layer. For this, the sensing probe was dipped into 3:1 (v/v) methanol and DI water solution for 6 min. After removing, the probe was kept overnight to dry. This completed the sensing probe fabrication process. To ensure the complete removal of template, dipping time of the probe in methanol and DI water solution was optimized in the further stage of the experiment. The corresponding probes with molecularly non-imprinted polymers (MWNTs@BSA-NIPs) were prepared in the same manner in the absence of template protein. Step wise pictorial representation of the probe fabrication and MIP is shown in figure 1 (a).

Experimental Set up

The experimental setup used for the characterization of the fiber optic SPR based protein sensor is shown in figure 1(b). It consists of a glass flow cell, tungsten halogen lamp source (Avalight-HAL) and a spectrometer (AVASPEC 3648). The flow cell made up of glass was used for fixing the sensor probe. The flow cell having the facility of inlet and removal of analyte solutions was fixed on a 3d-translational stage for proper adjustments and light coupling into the fiber probe. Before fixing the probe in the flow cell, both the ends of the probes were unclad and the tips were made sharp by a tungsten cutter and cleaned with DI water and acetone for fine light coupling from the source to the probe and from fiber to the spectrometer at the other end. Light from the polychromatic tungsten halogen lamp was launched in one end of the fiber using microscope objective. The evanescent wave of the light at the core-silver interface excites the surface plasmons at the silver-nanocomposite interface. The spectrum of the transmitted light exiting from the other end of the fiber was recorded by the spectrometer interfaced with a computer. To start the experiment, sample solution of given concentration was poured in the flow cell to record its SPR spectrum and hence the peak absorbance wavelength.

Surface morphology of MWCNTs using SEM

Surface morphology of uniformly dispersed and functionalized MWCNTs was analysed by SEM before and after removal of the template molecules. Figure 2(a) depicts the SEM image of MWCNTs dispersed in DI water. The cylindrical geometry of MWCNTs with high density can be clearly seen in this micrograph. The dispersed CNTs are seen as bundled tubes with very non-uniform dispersibility. Acid treatment of MWCNTs followed by functionalization

with MPTS provides evenly dispersed tubes with a bit shortened lengths as reported widely in literature and can be verified with surface morphology shown in figure 2(b). The SEM image of the MWCNTs@BSA-MIP core-shell is shown in figure 2(c). It shows the morphology of BSA immobilised CNTs engraved in polymeric mixture on a wider scale. When this is washed with methanol:DI solution, the morphology after removing BSA molecules from MWCNT@MIP layer is presented in figure 2 (d). A highly porous layer due to the removal of BSA molecules from the MWCNTs polymer matrix is obtained as can be seen from figure 2(d).

Results and Discussion

Sensing mechanism

The sensing mechanism of BSA is based on the change in the effective refractive index of the MWCNTs@BSA-MIP layer due to the binding of BSA molecules with the BSA imprinted sites created in the MWCNTs@ MIP layer. When BSA molecules comes in the domain of the imprinted sites, due to the complementary shape and size of the template sites in the monomer (MAA) layer, BSA molecules bind non-covalently with these imprinted sites as shown in fig. 1 (b). This will result in the change in the effective refractive index of the MIP layer and will result in a shift in the peak absorbance wavelength (λ_{peak}) in the absorbance spectrum. It may be noted that due to the presence of MWCNTs in the sensing medium, the absorbance spectrum was recorded. The peak absorbance wavelength is sensitive to the change in dielectric constant of the sensing medium. For each concentration of BSA, the number of binding sites attached with BSA differs, effective refractive index differs and hence the absorbance and peak absorbance wavelength also differs [33]. Hence, the sensing of BSA by MIP on MWCNT coated optical fiber is based on a combinational approach of molecular imprinting and surface plasmon resonance.

Optimization of probe parameters

Optimization of probe parameters were carried out to obtain the best performance of the MIP based BSA sensor. First, the concentration of BSA molecule for the creation of active sites in MIP layer was optimized. After that, the dipping period of the fiber into the MWCNT@BSA-MIP solution were optimized for the coating over the Ag coated fiber core. This is related to the thickness of sensing layer i.e MWCNT@BSA-MIP layer. Finally, the dipping time for the removal of template into methanol: DI solution was also optimized to ensure the complete removal of the template from the sensing layer.

Optimization of BSA concentration

In order to optimize the concentration of BSA in the fabrication of MWCNT@MIP layer for the high performance of the sensor, experiments were performed on the probes fabricated with different concentrations of BSA used for MIP layer. The number of active sites in the sensing layer is decided by the concentration of the template molecule used for the preparation of MWCNTs@MIP layer. This is also responsible for the final range in which the probe operates. Thus, for the presently considered range, five sensing probes were prepared with variation in BSA concentration from 5 to 25 mg/L. The SPR responses of each probe were recorded in the range of 0 to 350 ng/L concentration of protein sample solutions and the shift in peak absorption wavelength was determined from their SPR spectra. Fig. 3 (a) shows the representation of the shift in absorption peak for the probes fabricated with different concentrations of BSA in MWCNT@MIP layer. From the figure it is observed that the BSA concentration of 15 mg/L used in the probe fabrication gives the maximum shift of 73 nm in absorbance peak which is greater than the shift obtained for the probes fabricated with other concentrations of BSA. This is because the use of low concentration of BSA in the probe fabrication results in the creation of lower number of active sites in MWCNT@MIP layer and hence less binding of template molecule to the MWCNT@MIP layer or less shift in peak absorbance wavelength is obtained. For BSA concentration greater than 15 mg/L the shift in peak absorbance wavelength obtained is also less due to the limited surface area of the sensing region which results in a definite number of active sites available in the sensing layer. Further, the large concentration of BSA increases the disturbance in shape and size of the active sites in MIP layer. This results in lesser number of template molecules binding with the sensing surface and hence lesser shift in absorption peak is observed for BSA concentrations greater than 15 mg/L.

Optimization of dipping period for the coating of MWCNTs@BSA-MIP layer

The dipping period of the fiber in the MWCNTs@BSA-MIP solution was optimized for the coating of MWCNTs@BSA-MIP layer over Ag coated fiber core. The dipping period of the fiber decides the thickness of the sensing layer and the optimized thickness corresponds to the best performance of the sensor. It has been reported that the thickness of a dielectric layer over metal layer in a plasmonic sensor highly affects the electric field intensity at the interface of the sensing layer. The increase in electric field intensity increases the sensitivity of the sensor [32]. Thus, various probes were fabricated with different dipping time from 5 min to 30 min in MWCNTs@BSA-MIP solution of optimized BSA concentration (15 mg/L) while the dipping time for the template removal/unbinding was kept constant as 2 min. The variation of shift in λ_{peak} for BSA sample concentration change from 0 to 350 ng/L as a

function of dipping time is shown in figure 3(b). It is quite clear from figure that sensing probe possess maximum shift of 73nm in λ_{peak} for dipping period of 20 min. Thus, 20 min dipping period was the optimized period for optimum thickness of sensing layer over Ag coated fiber core. For the further confirmation of thickness corresponding to 20min dipping time, an optical profilometer was used and it was found to be around 1 μm.

Optimization of dipping period for removal of template

The last optimization was performed for the dipping time of the sensing probe in methanol: DI water (3:1 v/v) solution for the removal of template from the MWCNT@MIP layer. The dipping time in methanol:DI water solution is responsible for creating and controlling the cavities or imprinted sites on MWCNTs@MIP layer which affects the sensor probe performance. In this optimization, sensing probes were prepared using MWCNT@ MIP layer with optimized BSA concentration of 15 mg/L, optimized dipping period of 20 min for the coating of MWCNT@ MIP layer and different dipping periods (2 to 12 min) in methanol: DI water solution for the removal of BSA molecules. Figure 3(c) depicts the shifts in λ_{peak} for BSA sample concentration change from 0 to 350 ng/L as a function of removal time for the BSA unbinding from the MIP layer. It can be noted from the figure, the best performance of the sensor is obtained for the removal time of 6 min with 83 nm shift in λ_{peak} which implies that the maximum number of BSA molecules have been extracted without spoiling the imprints and the probe structure. A removal time of less than 6 min could not remove all the template molecules while the removal time greater than 6 min deteriorates the coating of MIP layer.

Effect of pH of BSA solution

The effect of pH of BSA solution on the performance of the optimized sensing probe has also been studied. BSA solutions were prepared in phosphate buffer with varying pH (5.0, 6.0, 7.0, 8.0 and 9.0). Figure 3 (d) shows the effect of pH of BSA solution on the shift in λ_{peak} for BSA concentration change from 0 to 350 ng/L. It may be seen that the shift in peak absorbance wavelength increases as the pH increases from 5 to 7 while it decreases as the pH is increased from 7. This is because of the highest stability of BSA and the MIP layer at pH 7.

Sensors probe characterization

After the optimization of all the parameters (BSA concentration for MWCNTs@BSA-MIP = 15 mg/L, dipping period for the coating = 20 min and the dipping period for the removal of BSA templates = 6 min), the final sensing probe was characterised using the setup shown in Fig. 1(b). BSA solutions with eight different concentrations in the range from 0 to 350 ng/L were poured into the flow cell successively to record their corresponding absorption spectra.

Sensing region of the probe was washed with DI water between two consecutive solutions to remove the essence of previous solution. Figure 4 (a) shows the absorption spectra of the optimized sensing probe for BSA concentrations in the range from 0 to 350 ng/L. It is quite clear from the figure that a shift in absorption spectrum towards higher wavelength is obtained for the increase in the concentration of BSA. The shift in absorption spectrum is due to the binding of BSA molecules with the active sites present in the MIP layer. These binding sites are active only for the specified target molecule because of the complementary shape and size of the molecule that can easily bind with the sites. The binding of template molecules results in the change in the dielectric constant of the MIP layer. Since the peak absorption wavelength is shifting towards the red wavelength it simply implies that the refractive index of the MIP layer increases due to the binding of BSA molecules [34]. The peak absorbance wavelength and its variation with BSA concentration is plotted in figure 4(b). For BSA concentration of 0 ng/L, absorption peak is obtained at 480 nm wavelength while for 350 ng/L concentration of BSA the absorption peak is obtained at 553 nm wavelength. A shift of about 73 nm in peak absorbance wavelength for the concentration change from 0 to 350 ng/L is observed. The data points are the experimental observations and have been fitted using a modified Langmuir isotherm. Langmuir isotherm is widely used for the characterisation of adsorption in the case of molecularly imprinted polymers [35]. The equation used for the fitting is

$$\lambda_{peak} = 480 + \frac{NKc}{1+Kc} \quad (1)$$

where N = 99.071 nm, K = 0.008698 L/ng, λ_{peak} is the peak absorbance wavelength in nm at concentration c in ng/L. The Langmuir equation has been modified to take into account the correction at zero concentration i.e. the peak absorbance wavelength at zero concentration is added to the Langmuir equation for zero correction. It can also be concluded from figure 4 (b) that the peak absorption wavelength tends to saturate at the higher concentration of BSA. The logic behind this trend is the availability of a finite number of active sites on the sensing layer for template the molecules, which allows the formation of a finite number of BSA imprints. At lower concentration, the number of binding sites per BSA molecule is maximum. As the BSA concentration increases, the available active sites start getting filled and a shift in peak absorption wavelength is observed. For higher concentration of BSA solutions, the maximum active sites are filled which results in the decrement in binding sites available per molecule and hence saturation of calibration curve as shown in figure 4(b).

The most basic and important parameter of a sensor is its sensitivity. For our fabricated sensing probe, it has been defined as the change in peak absorbance wavelength with respect to unit change in BSA concentration and therefore, it is calculated by taking the derivative of the calibration curve shown in figure 4(b) i.e. equation 1. Maximum sensitivity of the sensing probe has been found to be 0.862 nm/ngL^{-1}. The nature of the curve in figure 4(c), shows that the sensitivity decreases with the increase in BSA concentration. As mentioned above, this is due to the limited number of active sites available in the MIP layer.

To verify the role of MIP layer, control experiments were performed for each layer at the every step of the probe fabrication. Five different probes, having coatings of Ag layer alone, Ag/MWCNTs, Ag/MWCNT@NIP, Ag/MWCNTs@BSA-MIP and Ag/BSA-MIP were fabricated and their absorption spectra were recorded for the concentration range of BSA from 0 to 350 ng/L. The comparison of shift in peak absorbance wavelength for all the probes in the form of histogram is shown in figure 5(a). A shift of 10 nm in peak absorption wavelength was observed for bare silver coated probe. A small shift of 5 nm and 3nm were recorded for Ag/MWCNTs and Ag/MWCNT-NIP coated probe respectively. Significantly higher shift in the case of Ag/MWCNTs@MIP probe was observed for the same concentration change of BSA solution. This predicts the importance of molecular imprinting in the present approach. The control experiment with the probe having Ag/BSA-MIP is included to show the importance of the use of MWCNTs in the present study. The surface imprinting technique considerably increases the sensitivity due to the availability of more surface area and diffusion relaxation for proteins as compared to the bulk imprinting [19, 20]. Hence, a significant difference in the shift in peak absorbance wavelength for the two probes having Ag/MWCNTs@BSA-MIP and Ag/BSA-MIP layers can be seen.

Probe selectivity

Selectivity is a very crucial parameter of the sensor which decides its specificity for the tracing of desired analyte in a complex medium. MIP based sensors possess high selectivity due to complementary size and shape of template in the MIP layer as mentioned in the introduction. In order to check the selectivity of fabricated sensing probe, experiments with different analytes were performed. The analytes which can interfere with BSA detection and chosen for the selectivity tests are HSA, BHb (Bovine Hemoglobin), glucose, urea and dopamine. The first two analytes belong to protein family having similar nature and structure as BSA and the rest belong to different families. Figure 5(b) depicts the shift in λ_{peak} for the change in concentration different analytes from 0 to 350 ng/L. It can be observed that the

highest shift in λ_{peak} is observed for BSA while for the other analytes the shift is negligible. This shows highly selective nature of fabricated sensing probe for BSA. It can be concluded that the involvement of molecular imprinting technique for BSA sensing makes the sensor highly selective. Because the binding sites prepared in the MIP layer are complementary to the shape and size of BSA molecule, only BSA molecules interact with the binding sites present on the MIP layer. Any other molecule with different shape and size would not be able to bind with the active sites. Little shift in absorbance peak is due to the small interaction of other analytes with the functional monomer. It may noted that although single molecule templating cannot be demonstrated with SEM images, the selectivity of the device suggests that it was successful.

Repeatability

The repeatability of the finalized probe was checked by performing the experiments with BSA solutions of concentrations 0 and 350 ng/L in 4 cycles. First, the buffer (0 ng/L solution) was poured into the flow cell and its absorbance spectrum was recorded by the spectrometer. The buffer was then replaced by BSA solution of 350 ng/L concentration in the flow cell and its absorbance spectrum was recorded. These measurements were repeated four times. The peak absorbance wavelengths evaluated from all the absorbance spectra have been plotted with the number of cycles in fig 5(c). Table 1 shows the observed data for these four cycles and the percentage deviation in peak absorbance wavelength for the two extreme concentrations. It can be concluded that a negligible variation in peak absorbance wavelength (within 0.1%) is observed. Thus the sensor probe possesses high repeatability.

Response time

The response time of the sensor probe was investigated by measuring the absorbance as a function of time at a particular wavelength immediately after pouring the sample in the flow cell. To measure for the proposed probe, BSA solution of 250 ng/L concentration was injected into the flow cell and the absorbance spectrum was recorded with time. The variation of absorbance as a function of time at 550 nm wavelength for the sensing probe is shown in fig. 5(d). This figure shows that the absorbance value saturates in about 10 sec after the sample came in contact with the sensing probe. Thus the sensor has a response time of 10 s. No further change in absorbance was observed even after 30 min of pouring the BSA solution into the flow cell. This shows the highly stable nature of the proposed sensing probe.

Limit of detection

In addition to sensitivity, the performance of the sensing probe was also evaluated in terms of limit of detection (LOD) which can be determined as the lowest measurable concentration of

the analyte by the sensor. In the present study, it is based on the spectral resolution of the spectrometer and the sensitivity of the sensing probe near zero concentration of the analyte [22]. It can be mathematically expressed as $C_{LOD} = \Delta\lambda_{resolution}/S_{C=0}$; where C_{LOD} represents the limit of detection of the sensor, stands for the spectrometer resolution and S represents the sensor sensitivity near blank (zero) concentration. The sensitivity, near zero concentration, according to Fig. 4(c), is 0.862 nm/ngL^{-1} and the spectrometer resolution is 0.333 nm. The value of LOD for the present sensor was calculated to be 0.386 ng/L. To verify the advantage of present approach, a comparison of the detection limit of the proposed sensor with the previously reported values by the other methods for BSA detection is shown in Table 2. It can be noticed from the table that the proposed sensor possesses the lowest detection limit as compared to other methods.

Conclusion

To summarise, a novel probe has been fabricated and calibrated for the sensing of BSA in the concentration range 0-350ng/L integrating the effect of FOSPR and MIP. The probe has been realised using Ag thin film deposited using thermal evaporation and CNT based MIP platform created by dip coating. The probe has been characterised by recording absorbance spectrum for each BSA concentration. The calibration parameter i.e peak absorbance wavelength increases with increase in the concentration of BSA and probe has been found to be most sensitive for lowest concentration. Molecular imprinting technique ensures the selectivity over various similar analytes considered for selectivity test. Various optimisation parameters like dipping time for deposition and template removal, pH and effect of each layer have been explored in detail. The stability and repeatability of the probe has been checked by repeating the experiments. Further, the probe has a very fast response time of 10 s and lowest LOD compared to the other sensors reported in literature with other advantages like real time online monitoring due to the use of optical fiber.

References

1. Preejith P V, Lim C S, Kishen A, John M S and Asundi A 2003 Total protein measurement using a fiber-optic evanescent wave-based biosensor *Biotech. Lett.* **25** 105–10
2. Wang Y and Wei T X 2013 Surface plasmon resonance sensor chips for the recognition of bovine serum albumin via electropolymerized molecularly imprinted polymers *Chinese Chem. Lett.* **24** 813–6
3. Zhang L L, Ma F F, Kuanga Y F, Cheng S, Long Y F and Xiao Q G 2016 Highly sensitive detection of bovine serum albumin based on the aggregation of triangular silver nano particles *Spectrochim. Acta Part A: Mol. and Biomol. Spectros.***154** 98–102
4. Jinghua Y, Fuwei W, Congcong Z, Mei Y, Xiaona Z and Shaowei W 2010 Molecularly imprinted polymeric microspheres for determination of bovine serum albumin based on flow injection chemiluminescence sensor *Biosens. Bioelect.* **26** 632–7
5. Leung A, Shankar P M and Mutharasan R 2007 Real-time monitoring of bovine serum albumin at femtogram/mL levels on antibody-immobilized tapered fibers *Sens. Actuat. B* **123** 888–95
6. Bradford M M 1976 A rapid and sensitive method for the quantification of microgram quantities of protein utilizing the principle of protein-dye binding *Anal. Biochem.* **72** 248-54
7. Lin J Q, Chen R, Feng S Y, Pan J J and Li Y Z 2011 A novel blood plasma analysis technique combining membrane electrophoresis with silver nanoparticle-based SERS spectroscopy for potential applications in noninvasive cancer detection *Nanomed. Nanotechnol. Biol. Med.* **7** 655–63
8. Cui C J, Cai W S and Shao X G 2013 Near-infrared diffuse reflectance spectroscopy with sample spots and chemometrics for fast determination of bovine serum albumin in micro-volume samples *Chin. Chem. Lett.* **24** 67–9

9. Zhang X W, Zhao F L and Liu K A 2001 Fluorometric method for the micro determination of protein using indigo carmine *Microchem. J.* **68** 53–9
10. Wei Q, Wu D, Du B, Li Z J and Huo Y Q 2006 A spectrophotometric method for determination of total proteins in cow milk powder samples using the o-nitrophenylfluorone/Mo(VI) complex *J. Food Compos. Anal.* **19** 76–82
11. Cai1 D, Ren L, Zhao H, Xu C, Zhang L, Yu Y, Wang H, Lan Y, Roberts M F, Chuang J, Naughton M J, Ren Z, and Chiles T C 2010 A molecular imprint nanosensor for ultrasensitive detection of proteins *Nat. Nanotechnol.* **5** 597–601
12. Gupta B D, Shrivastav A M and Usha S P 2016 Surface plasmon resonance-based fiber optic sensors utilizing molecular imprinting *Sensors* **16** 1381
13. Vlatakis G, Andersson L I, Muller R and Mosbach K 1993 Drug assay using antibody mimics made by molecular imprinting *Nature* **361** 645–7
14. Wulff G 1995 Molecular imprinting in cross-linked materials with the aid of molecular templates-a way towards artificial antibodies *Angew. Chem. Int. Ed. Engl.* **34** 1812–32
15. Zhang Z, Yang X, Chen X, Zhang M, Luo L, Peng M and Yao S 2011 Novel magnetic bovine serum albumin imprinted polymers with a matrix of carbon nanotubes, and their application to protein separation *Anal. Bioanal. Chem.* **401** 2855–63
16. Lv Y, Tan T, Svec F 2013 Molecular imprinting of proteins in polymers attached to the surface of nanomaterials for selective recognition of biomacromolecules *Biotech. Adv.* **31** 1172-86
17. Kempe M, Glad M and Mosbach K. 1995 An approach towards surface imprinting using the enzyme ribonuclease A *J. Mol. Recognit.* **8** 35-9
18. Shi H, Tsai W B, Garrison M D, Ferrari S and Ratner B D 1999 Template-imprinted nanostructured surfaces for protein recognition *Nature* **398** 593-7
19. Prasad B B, Madhuri R, Tiwari M P, Sharma P S 2010 Imprinting molecular recognition sites on multiwalled carbon nanotubes surface for electrochemical detection of insulin in real samples *Electrochim. Acta* **55** 9146–56
20. Kan X, Zhao Y, Geng Z, Wang Z, Zhu J J 2008 Composites of multiwalled carbon nanotubes and molecularly imprinted polymers for dopamine recognition *J. Phys. Chem C* **112** 4849–54
21. Ding H, Chen R, Liu M, Huang R, Du Y, Huang C, Yu X, Feng X and Liu F 2016 Preparation and characterization of biocompatible molecularly imprinted poly(ionic liquid) films on the surface of multi-walled carbon nanotubes *RSC Adv.* **6** 43526

22. Pathak A, Parveen S and Gupta B D 2017 Fibre Optic SPR Sensor Using Functionalized CNTs for the Detection of SMX: Comparison with Enzymatic Approach *Plasmonics* DOI:10.1007/s11468-017-0499-z
23. Agrawal H, Shrivastav A M and Gupta B D 2016 Surface plasmon resonance based optical fiber sensor for atrazine detection using molecular imprinting technique *Sens. Actuat. B* **227** 204–11
24. Sharma A K, Jha R and Gupta B D 2007 Fiber optic sensors based on surface plasmon resonance: a comprehensive review *IEEE Sens. J.* **7** 979761
25. Ma P C, Siddiqui N A, Marom G and Kim J K 2010 Dispersion and functionalization of carbon nanotubes for polymer-based nanocomposites: a review *Composites: Part A* **41** 1345–67
26. Ortega-Munoz M, Morales-Sanfrutos J, Megia-Fernandez A, Lopez-Jaramillo F J, Hernandez-Mateo F and Santoyo-Gonzalez F 2010 Vinyl sulfone functionalized silica: a ‘‘ready to use’’ pre-activated material for immobilization of biomolecules *J. Mater. Chem.* **20** 7189–96
27. Mosa J, Duran A, Aparicio M 2015 Sulfonic acid-functionalized hybrid organiceinorganic proton exchange membranes synthesized by solegel using 3-mercaptopropyl trimethoxysilane (MPTMS) *J. of Power Sources* **297** 208-16
28. Lopez-Jaramillo F J, Hernandez-Mateo F and Santoyo-Gonzalez F 2012 Vinyl Sulfone: A Multi-Purpose Function in Proteomics *Integrative Proteomics* eds. H C E Leung et al (Intech)
29. Bag D S, Dubey R, Zhang N, Xie J, Varadan V K, Lal D and Mathur G N 2004 Chemical functionalization of carbon nanotubes with 3-methacryloxypropyltrimethoxysilane (3-MPTS) *Smart Mat. Struct.* **13** 1263-7
30. Hu C H and Chou T C 2009 Albumin molecularly imprinted polymer with high template affinity-prepared by systematic optimization in mixed organic/aqueous media *Microchem. J.* **91** 53–8.
31. Zhang J, Ma J, Yue X , Bu X and Han Y 2012 Preparation and characterization of molecularly imprinted polymer of bovine serum albumin *J. Appl. Polym. Sci.* **124** 723-8.
32. Shalabney A and Abdulhalim I 2010 Electromagnetic fields distribution in multilayer thin film structures and the origin of sensitivity enhancement in surface Plasmon resonance sensors *Sens. Actuat. A* **159** 24-32
33. Shrivastav A M, Usha S P and Gupta B D 2016 Fiber optic profenofos sensor based on surface plasmon resonance technique and molecular imprinting *Biosens. Bioelect.* **79** 150–7

34. Jorgenson R C and Yee S S 1993 A fiber-optic chemical sensor based on surface plasmon resonance, *Sens. Actuat. B* **12** 213-20
35. Umpleby R J, Baxter S C, Chen Y, Shah R N, and Shimizu K D 2001 Characterization of molecularly imprinted polymers with the Langmuir-Freundlich isotherm *Anal. Chem.* **73** 4584-91
36. Peng L, Li C Y, Xue H B and Zhan G Q 2010 Ultrasensitive determination of serum albumin using resonance light scattering based on ZnS-polyacrylic acid nanoparticles. *Spectrochim. Acta A Mol. Biomol. Spect.* **75** 1497-500
37. Chen H J, Zhang Z H, Luo L J and Yao S Z 2012 Surface-imprinted chitosan-coated magnetic nanoparticles modified multi-walled carbon nanotubes biosensor for detection of bovine serum albumin *Sens. Actuat. B* **163** 76– 83
38. Zhang X M, Song C J, Chen L L, Zhang K, Fu A H, Jin B Q, Zhang Z J and Yang K 2011 A novel immunoassay for residual bovine serum albumin (BSA) in vaccines using laser-induced fluorescence millimeter sensor array detection platform *Biosens. Bioelectron.* **26** 3958-61
39. Xu X J, Huang J, Li J J, Yan J W, Qin J G and Li Z 2011 A graphene oxide-based AIE biosensor with high selectivity toward bovine serum albumin *Chem. Commun.* **47** 12385-87
40. Chen H J, Zhang Z H, Xie D, Cai R, Chen X, Liu Y N and Yao S Z 2012 Surface-imprinting sensor based on carbon nanotubes/graphene composite for determination of bovine serum albumin *Electroanal.* **24** 2109 –16.

Figure captions

1. (a) Schematic of steps involved in probe synthesis, and (b) experimental set-up used for the sensing of BSA using SPR and MIP platform on MWCNTs, and sensing mechanism.
2. SEM images of (a) MWCNTs as obtained, (b) Functionalised MWCNTs, (c) BSA imprinted MIP on MWCNTs, and (d) MIP layer after the removal of template (BSA) molecules. The SEM images from c to d suggest the template removal but the resolution is inadequate to demonstrate the single-molecule templating.
3. Optimisation of (a) BSA concentration in the imprinted layer, (b) dipping time for the coating of MIP layer over silver coated probe, (c) dipping time for the template removal, and (d) pH of BSA solutions.
4. (a) SPR absorption spectra, (b) peak absorbance wavelength, and (c) sensitivity of fiber optic SPR and MIP based probe using MWCNTs for BSA detection.
5. (a) Control experiments plots for various probes underlining the importance of MIP, (b) selectivity of MIP based probe for BSA over other similar interfering analytes, (c) response time of the sensor probe for BSA, and (d) repeatability of the probe for 4 cycles to show consistency in peak absorbance wavelength

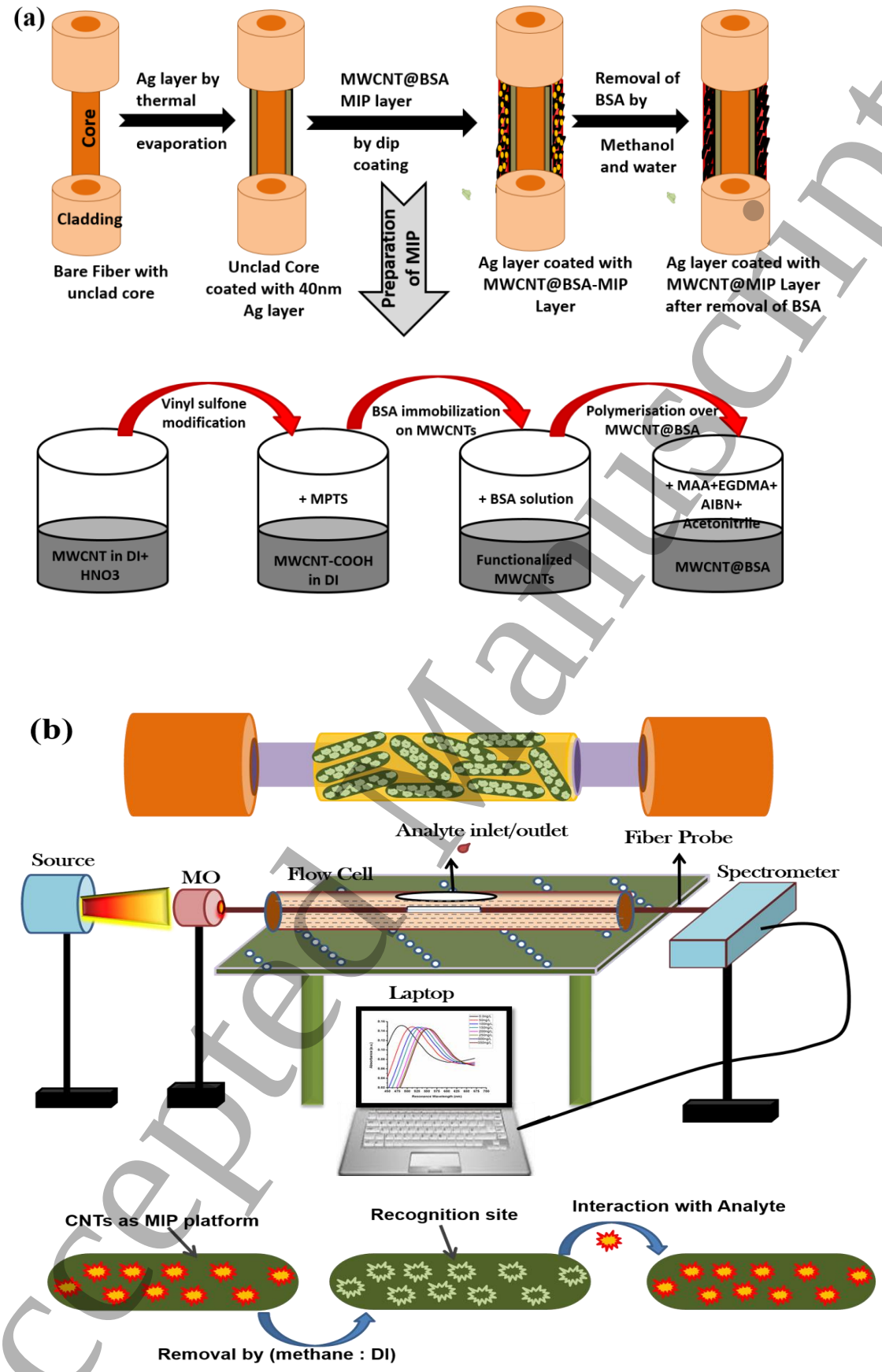

Figure 1

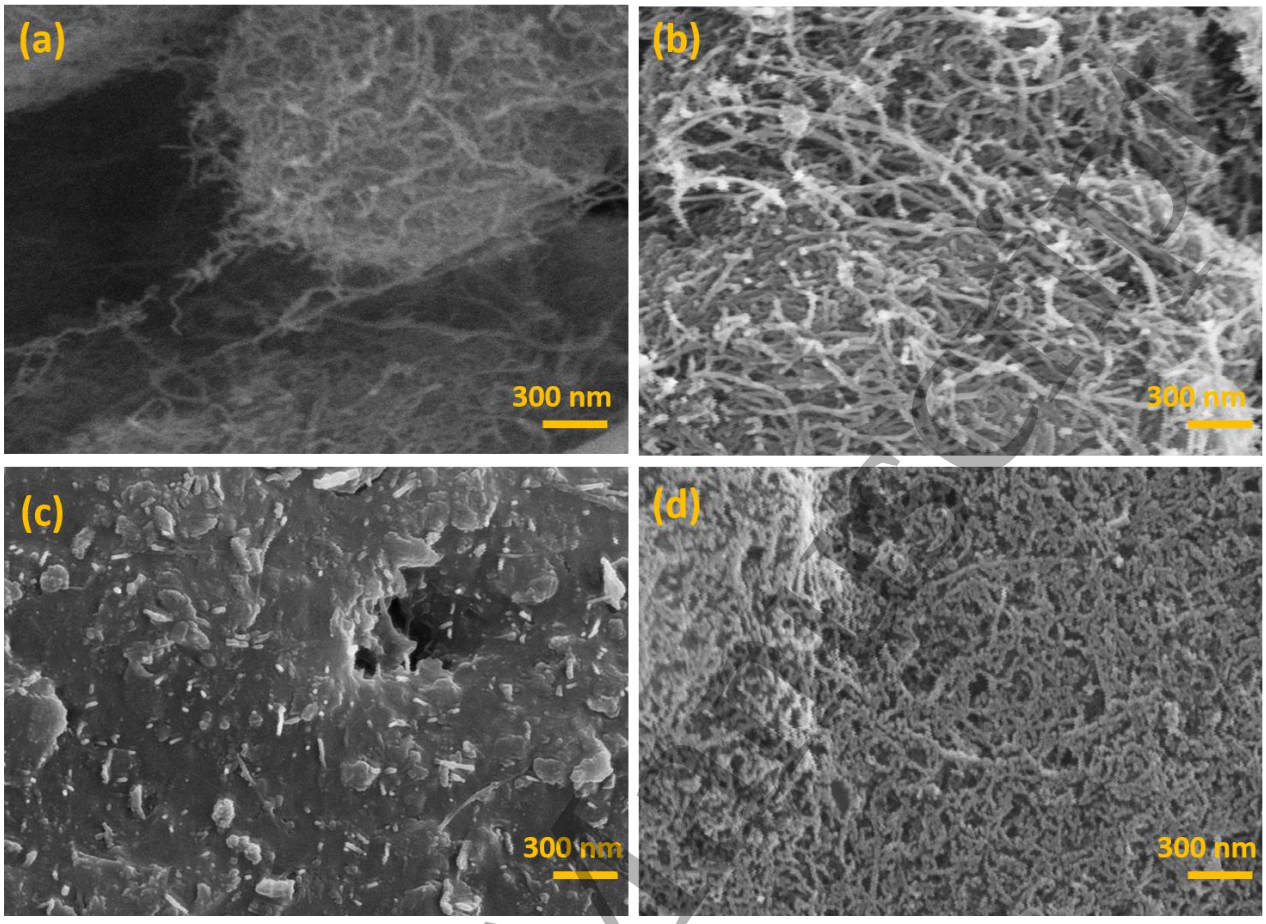

Figure 2

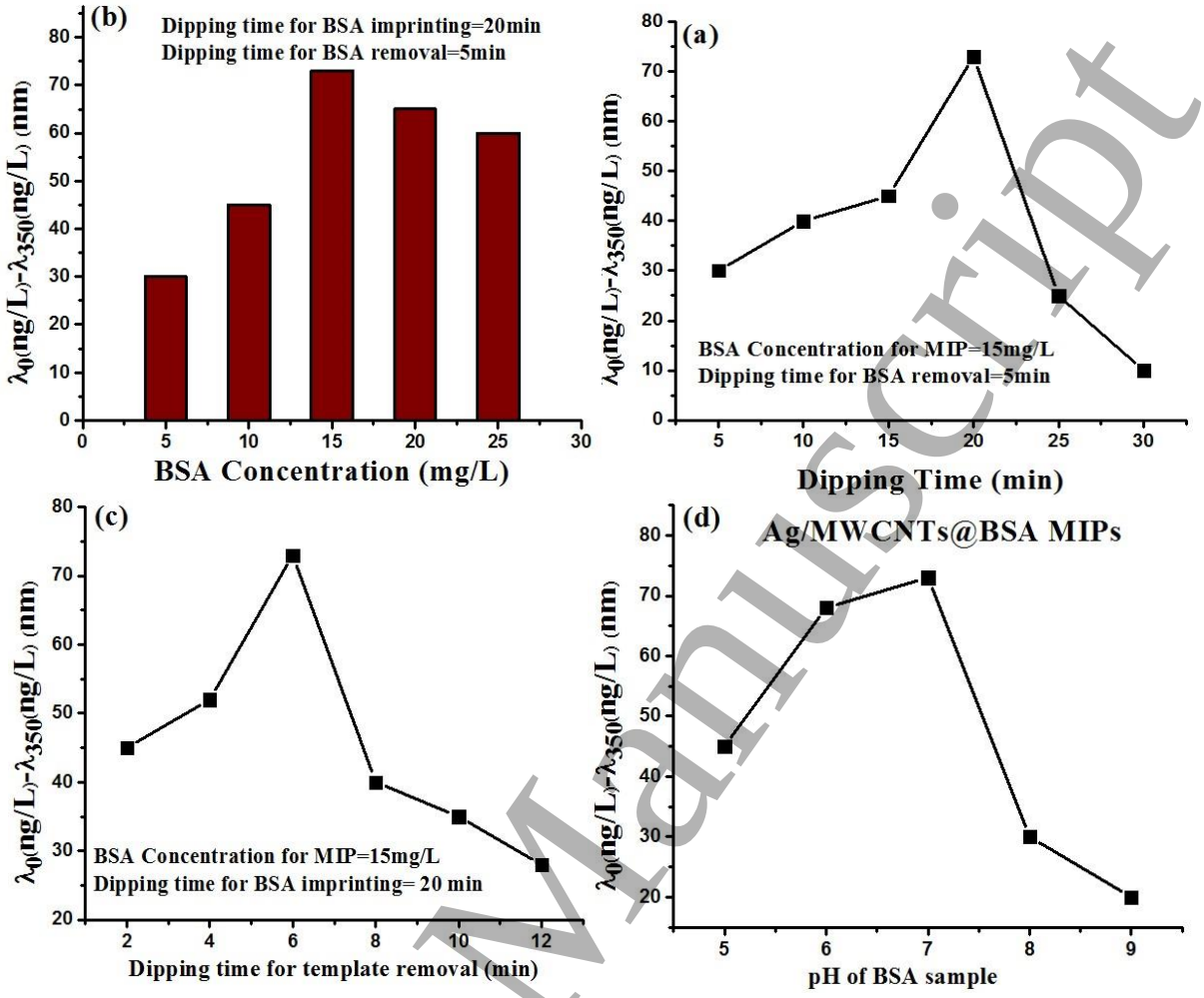

Figure 3

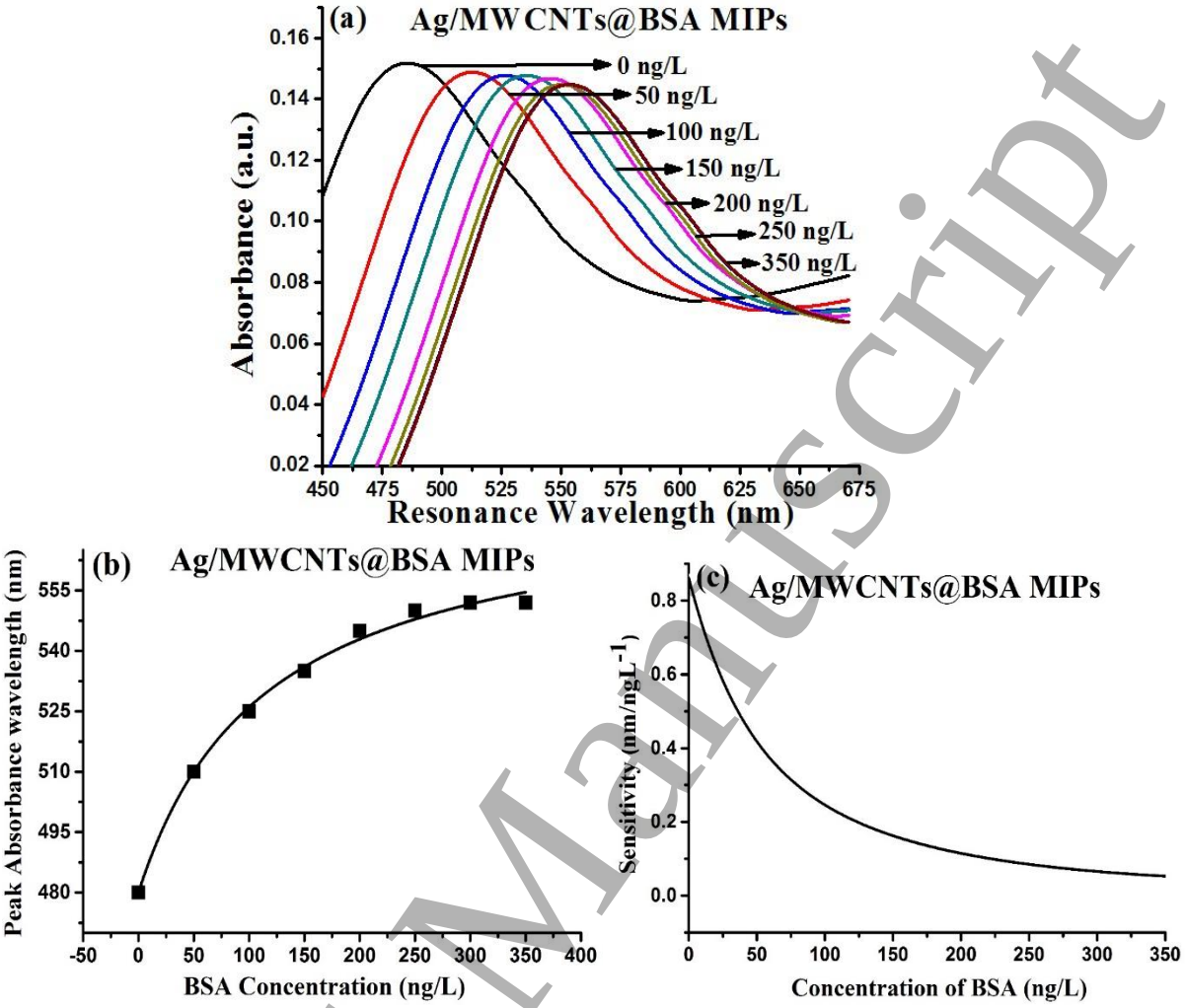

Figure 4

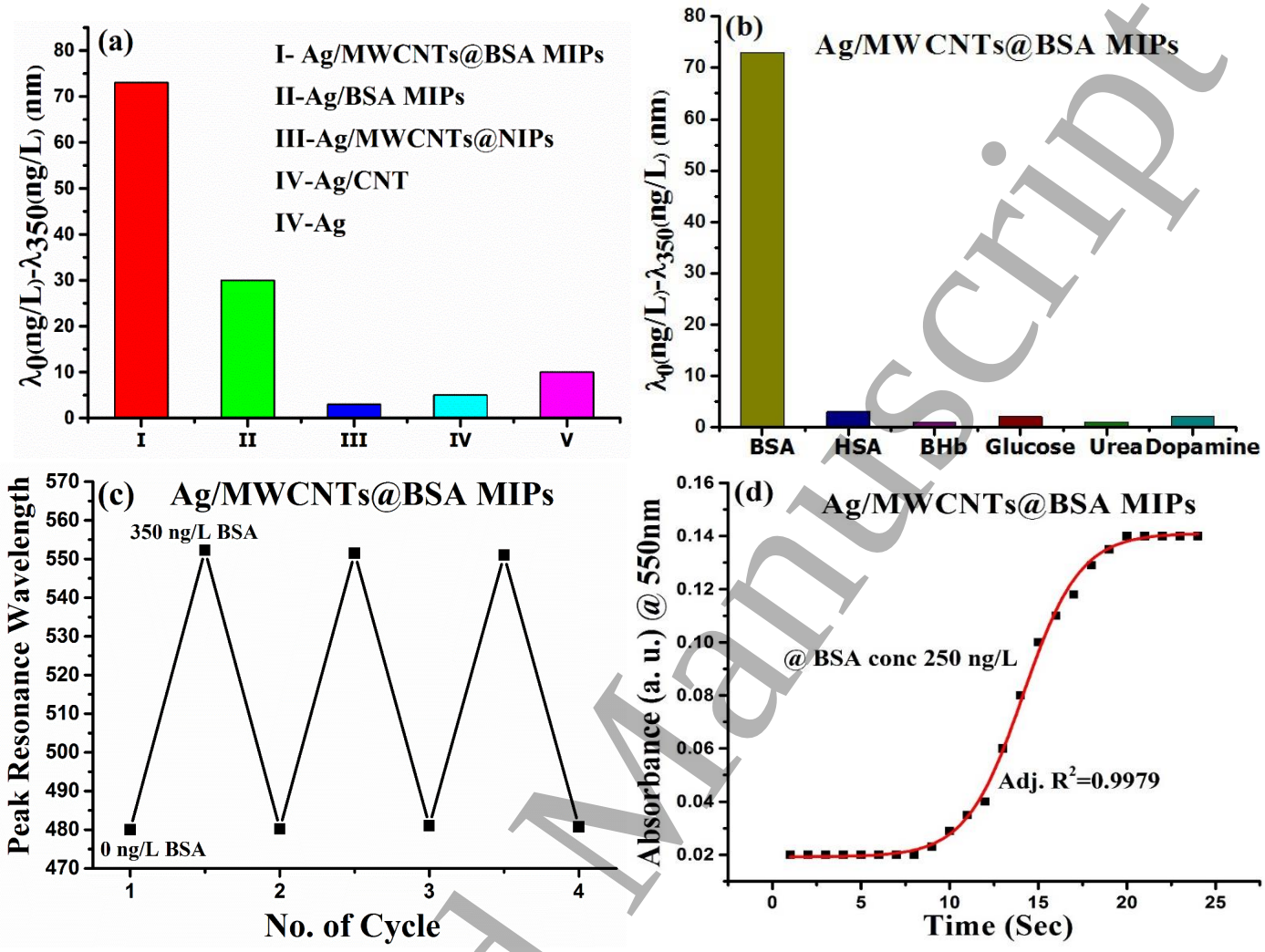

Figure 5

Table 1. Peak absorbance wavelengths at two extreme concentrations for 4 cycles of repeated measurements with percentage deviation

Cycle	λ_{peak} (0 ng/L)	% Deviation	λ_{peak} (350 ng/L)	% Deviation
1	480.0		552.0	
2	480.2	0.07%	551.5	0.09%
3	481.0		551.0	
4	480.7			

Table 2. Comparison of limit of detection of present sensor with other BSA sensors reported in the literature

Technique	**Operating range**	**LOD**	**Reference**
Electropolymerized/ MIP	0.02-0.8 mg/mL	0.02 mg/mL	[1]
Spectrophotometric-triangular Ag NPs	1-100 mg/mL	0.5 ng/mL	[2]
Resonance light scattering	10^{-9}-1.2×10^{-7} g/mL	5×10^{-10} g/mL	[36]
DPV- MIP chitosan coated magnetic nanoparticles modified CNTs	10^{-4}-10^{-10} g/mL	28 ng/L	[37]
Fluorescence millimetre array	10^{-7}-1.2×10^{-9} g/mL	3×10^{-10} g/mL	[38]
Flow injection chemiluminescence - MIP microspheres	10 -5000 ng/mL	1.5 ng/mL	[4]
Fluorescence spectra	6×10^{-5}-0 g/mL	4×10^{-7} g/mL	[39]
MIP-graphene/CNT nanocomposite	10^{-10}-10^{-4} g/mL	62 ng/L	[40]
SPR-Ag/MWCNTs@MIP-BSA	0-350 ng/L	0.386 ng/L	Present Study